Int. J. Solids Structures Vol. 25, No. 5, pp. 527–538, 1989
Printed in Great Britain.

0020–7683/89 $3.00 + .00

BOUNDARY ELEMENT IMPLICIT DIFFERENTIATION EQUATIONS FOR DESIGN SENSITIVITIES OF AXISYMMETRIC STRUCTURES

SUNIL SAIGAL†, J. T. BORGGAARD and J. H. KANE
Mechanical Engineering Department, Worcester Polytechnic Institute, Worcester, MA 01609, U.S.A.

(*Received* 26 *May* 1988; *in revised form* 23 *September* 1988)

Abstract—Design sensitivity analysis of axisymmetric elastic media is formulated using boundary elements. The kernels for sensitivity matrices are obtained through implicit differentiation of the corresponding boundary element elasticity kernels. The singular terms are obtained by applying the boundary displacements and tractions, and their respective sensitivities for the rigid body motion mode and the inflation mode. The equations for the recovery of sensitivities of axisymmetric boundary stresses are presented. As a check on accuracy, the approach is applied to a series of examples for which analytical elasticity solutions are available. The predictions for both displacement- and stress-sensitivities are accurate. Additional examples are provided to demonstrate the versatility of the present approach.

INTRODUCTION

Many axisymmetric components, such as fan, compressor, and turbine disks in gas turbine engines, are employed in the design of high performance aerospace, automotive and other components. The determination of optimal shapes of such critical components is of obvious importance to the industry. The tools developed for such applications must be economical and efficient to be of practical utility. The boundary integral equation method described in texts by, among others, Barnerjee and Butterfield (1981) and Brebbia *et al.* (1984), provides the possibility of an accurate analysis tool for axisymmetric components with computing costs that are significantly less than those for axisymmetric finite element analysis as noted by Cruse *et al.* (1977). A survey of research efforts for the structural analysis of axisymmetric problems has been given by Bakr (1985).

The boundary element method also offers significant advantages for the efficient computation of response design sensitivities as noted by Saigal *et al.* (1989). This method has recently been employed for applications, such as structural analysis, heat transfer, potential problems and aerodynamics. A survey of such efforts was given by Mota Soares and Choi (1986). In the area of sensitivity analysis of elastic continua, the research efforts to date have been directed towards two-dimensional plane elasticity problems. Kane and Saigal (1988) presented the implicit differentiation formulation for sensitivity analysis using discontinuous boundary elements. This formulation was extended to continuous elements by Saigal *et al.* (1989). A shape optimization system based on this formulation has been developed by Saigal and Kane (1989). Wu (1986) employed a finite-difference scheme to obtain the derivative of the system matrices used in structural sensitivity analysis. Barone and Yang (1988) developed a direct differentiation approach of the relevant BEM equations for 2D problems followed by the discretization of these equations. Their method is a general one for 2D problems and they determined the sensitivities around the elliptical hole using this formulation. The research concerning the shape sensitivity analysis of axisymmetric elastic media has, however, not been reported in the literature so far.

The present paper presents a boundary element formulation for the design sensitivity analysis of axisymmetric continua. The sensitivity equations are first obtained by the implicit differentiation of the discretized axisymmetric boundary element equations. The numerical evaluation of the resulting integrals involving partial derivatives of the fundamental solutions is discussed. The cases of a rigid body mode, and an inflation mode, respectively, are

† To whom all correspondence should be addressed.

used for the evaluation of the singular terms. This technique is similar to the one available in the literature for the evaluation of axisymmetric analysis integrals and shown by Sarihan and Mukherjee (1982). Numerical examples are presented and compared to analytical solutions when available to test the accuracy, and to demonstrate the validity of the present formulations.

AXISYMMETRIC BOUNDARY ELEMENT ANALYSIS

A brief description of the axisymmetric boundary element formulation for linear elasticity is given here to introduce the notation used. A detailed discussion of this formulation may be found in, for example, the text by Banerjee and Butterfield (1981).

The boundary integral equations can be obtained from the principle of virtual work and Betti's reciprocal law as

$$\int_\Gamma T_{ik} u_i \, d\Gamma + \int_\Omega f_{ik} u_i \, d\Omega = \int_\Gamma T_i u_{ik} \, d\Gamma + \int_\Omega f_i u_{ik} \, d\Omega. \tag{1}$$

u_{ik} and T_{ik} are the axisymmetric fundamental solutions for the displacements and the tractions, respectively. The kernel functions u_{ik} and T_{ik} are the displacement and traction solutions, respectively, in the direction, i, due to a unit ring load in the direction, k. f_i are the body forces acting on the axisymmetric body. In this study, torsional loading and body forces are neglected. The resulting equation is then treated using a surface discretization. After discretization, the boundary element equations can be written in matrix form as

$$[A]\{u\} = [B]\{T\} \tag{2}$$

where

$$\begin{bmatrix} A_{rr} & A_{rz} \\ A_{zr} & A_{zz} \end{bmatrix}_{ij} = \int_a \begin{bmatrix} T_{rr} & T_{zr} \\ T_{rz} & T_{zz} \end{bmatrix}_{ij} [H] J \, da$$

$$\begin{bmatrix} B_{rr} & B_{rz} \\ B_{zr} & B_{zz} \end{bmatrix}_{ij} = \int_a \begin{bmatrix} u_{rr} & u_{zr} \\ u_{rz} & u_{zz} \end{bmatrix}_{ij} [H] J \, da \quad i, j = 1, 2, \ldots, N. \tag{3}$$

N is the number of degrees-of-freedom (d.o.f.); $[H]$ is the matrix of interpolation functions, $h^{(i)}(a)$, acting on the d.o.f.s associated with a given element; a is the isoparametric coordinate; and J is the Jacobian.

A singular formulation was used in the present study leading to singular integrals. The numerical evaluation of these singular integrals was avoided using the special cases of deformation in the rigid body mode and the inflation mode, respectively. From the rigid body mode condition

$$(A_{rz})_{ii} = -\sum_{\substack{j=1 \\ j \neq i}}^{N} (A_{rz})_{ij}, \quad (A_{zz}) = -\sum_{\substack{j=1 \\ j \neq i}}^{N} (A_{zz})_{ij}. \tag{4}$$

The inflation mode is obtained from the conditions

$$T_r = n_r, \quad T_z = 2\nu n_z, \quad u_r = r(1-2\nu)(1+\nu)/E, \quad \text{and} \quad u_z = 0. \tag{5}$$

n_r and n_z are the components of the normal in the r and z directions, respectively. ν and E are Poisson's ratio and Young's modulus of elasticity, respectively. This yields the remaining diagonal terms of the boundary element matrix $[A]$ from

$$(A_{rr})_{ii}(u_r)_i = \sum_{j=1}^{N} [B_{rr}B_{rz}]_{ij}[T_r T_z]_j^T - \sum_{\substack{j=1 \\ j\neq i}}^{N} [A_{rr}A_{rz}]_{ij}[u_r u_z]_j^T - (A_{rz})_{ii}(u_z)_i$$

$$(A_{zr})_{ii}(u_r)_i = \sum_{j=1}^{N} [B_{zr}B_{zz}]_{ij}[T_r T_z]_j^T - \sum_{\substack{j=1 \\ j\neq i}}^{N} [A_{zr}A_{zz}]_{ij}[u_r u_z]_j^T - (A_{zz})_{ii}(u_z)_i. \quad (6)$$

The terms $(A_{rz})_{ii}(u_z)_i$ and $(A_{zz})_{ii}(u_z)_i$ on the right hand side in eqns (6) are both zero for the present inflation mode since $u_z = 0$ for this mode. The errors introduced due to the row sum property in eqn (4) thus do not contribute to the evaluation of terms using eqns (6). The boundary conditions are applied to eqns (2) and these equations are then rewritten by bringing the unknown quantities on the left hand side and known quantities on the right hand side as

$$[\bar{A}]\{y\} = \{b\} \quad (7)$$

where $\{y\}$ is the vector containing the unknown displacements and tractions. On obtaining the unknown displacements and tractions using eqn (7), the complete stress tensor is obtained by substituting these quantities in the stress recovery expressions. These expressions may be found in, among others, the text by Bakr (1985).

AXISYMMETRIC DESIGN SENSITIVITY FORMULATIONS

Displacement and traction sensitivities

The design sensitivities determine the effect of variation of design parameters on the response of the model. Differentiating the discretized boundary element eqns (2) with respect to the design variable, X_L, we get

$$[A]_{,L}\{u\} + [A]\{u\}_{,L} = [B]_{,L}\{T\} + [B]\{T\}_{,L} \quad (8)$$

where $[*]_{,L}$ denotes the partial derivative of $[*]$ with respect to X_L. Equation (8) can be rearranged in the form

$$[A]\{u\}_{,L} = [B]\{T\}_{,L} + \{c\} \quad (9)$$

where

$$\{c\} = [B]_{,L}\{T\} - [A]_{,L}\{u\}.$$

The vector $\{c\}$ in the above equation is known since the unknown displacements and tractions are determined from eqn (7). Equation (9) is now rearranged to write the unknown displacement- and traction-sensitivities on the left hand side. It is noted here that the sensitivities corresponding to the specified displacements and tractions are known. The rearrangement of eqn (9) will then require the same column exchange as was required in writing eqn (7). Equation (9) is written in rearranged form as

$$[\bar{A}]\{y\}_{,L} = \{\bar{b}\} \quad (10)$$

where $\{y\}_{,L}$ is the vector of unknown displacement- and traction-sensitivities and is obtained through the solution of eqn (10). Notice that this equation has the same left hand side matrix, $[\bar{A}]$, as eqn (7). The triangular factorization of $[\bar{A}]$ obtained for the solution of eqn (7) can then be saved and reused for the solution of eqn (10). This feature of the implicit differentiation formulation leads to considerable computational economy.

The matrices $[A]_{,L}$ and $[B]_{,L}$ in eqn (8) are determined by performing implicit differentiation of eqn (3) as

$$\begin{bmatrix} A_{rr,L} & A_{rz,L} \\ A_{zr,L} & A_{zz,L} \end{bmatrix}_{ij} = \int_0^1 \left\{ \begin{bmatrix} T_{rr,L} & T_{zr,L} \\ T_{rz,L} & T_{zz,L} \end{bmatrix}_{ij} [H] J + \begin{bmatrix} T_{rr} & T_{zr} \\ T_{rz} & T_{zz} \end{bmatrix}_{ij} [H] J_{,L} \right\} \mathrm{d}a$$

$$\begin{bmatrix} B_{rr,L} & B_{rz,L} \\ B_{zr,L} & B_{zz,L} \end{bmatrix}_{ij} = \int_0^1 \left\{ \begin{bmatrix} u_{rr,L} & u_{zr,L} \\ u_{rz,L} & u_{zz,L} \end{bmatrix}_{ij} [H] J + \begin{bmatrix} u_{rr} & u_{zr} \\ u_{rz} & u_{zz} \end{bmatrix}_{ij} [H] J_{,L} \right\} \mathrm{d}a. \tag{11}$$

$u_{ij,L}$ and $T_{ij,L}$ are the partial derivatives of the kernel functions, u_{ij} and T_{ij}, respectively, with respect to the design variable X_L. These expressions are given in the Appendix. The sensitivities of kernel functions $u_{ij,L}$ and $T_{ij,L}$ require the sensitivities of geometric quantities ($r_{,L}$; $z_{,L}$; $n_{r,L}$; $n_{z,L}$; etc.) as seen from equations in the Appendix. To obtain these quantities, the original mesh is first perturbed through a change in the design variable X_L to obtain a new mesh. Forward-difference relationships are then applied between the original and the new mesh. The sensitivity of the Jacobian, $J_{,L}$, with respect to X_L is obtained as

$$J_{,L} = \frac{1}{J}[r_{,a} r_{,aL} + z_{,a} z_{,aL}]$$

where

$$r_{,a} = h_{,a}^{(i)} r^{(i)}, \quad r_{,aL} = h_{,a}^{(i)} r_{,L}^{(i)}, \quad z_{,a} = h_{,a}^{(i)} z^{(i)}, \quad z_{,aL} = h_{,a}^{(i)} z_{,L}^{(i)}.$$

The determination of the diagonal terms of the sensitivity matrices $[A]_{,L}$ and $[B]_{,L}$ requires the evaluation of singular integrals. These terms are evaluated by using the special cases of deformation in a rigid body mode and an inflation mode, respectively, similar to the evaluation of the diagonal terms of the boundary element matrices $[A]$ and $[B]$. Consider first a rigid body motion in the z direction given by: $u_r = t_r = t_z = 0$, and u_z = constant. The sensitivities of all displacements and tractions are equal to zero for this case. Substituting these conditions in eqn (8) leads to

$$(A_{rz,L})_{ii} = -\sum_{\substack{j=1 \\ j \neq i}}^{N} (A_{rz,L})_{ij}, \quad (A_{zz,L})_{ii} = -\sum_{\substack{j=1 \\ j \neq i}}^{N} (A_{zz,L})_{ij}. \tag{12}$$

Consider next the inflation mode conditions given by eqn (5). The corresponding sensitivities are given as:

$$T_{r,L} = n_{r,L}, \quad T_{z,L} = 2\upsilon n_{z,L}, \quad u_{r,L} = \frac{(1-2\upsilon)(1+\upsilon)}{E} r_{,L}, \quad u_{z,L} = 0. \tag{13}$$

The remaining diagonal terms are then obtained from

$$(A_{rr,L})_{ii}(u_r)_i = -(A_{rr})_{ii}(u_{r,L})_i + \sum_{j=1}^{N} [B_{rr,L} B_{rz,L}]_{ij} [T_r T_z]_j^T + \sum_{j=1}^{N} [B_{rr} B_{rz}]_{ij} [T_{r,L} T_{z,L}]_j^T - \sum_{\substack{j=1 \\ j \neq i}}^{N} (A_{rr,L})_{ij} (u_r)_j - \sum_{\substack{j=1 \\ j \neq i}}^{N} (A_{rr})_{ij} (u_{r,L})_j$$

and

$$(A_{zr,L})_{ii}(u_r)_i = -(A_{zr})_{ii}(u_{r,L})_i + \sum_{j=1}^{N} [B_{zr,L} B_{zz,L}]_{ij} [T_r T_z]_j^T + \sum_{j=1}^{N} [B_{zr} B_{zz}]_{ij} [T_{r,L} T_{z,L}]_j^T - \sum_{\substack{j=1 \\ j \neq i}}^{N} (A_{zr,L})_{ij} (u_r)_j - \sum_{\substack{j=1 \\ j \neq i}}^{N} (A_{zr})_{ij} (u_{r,L})_j. \tag{14}$$

This completes the formulation of the boundary element sensitivity matrices which are required for the solution of the sensitivity vector $\{y\}_{,L}$ in eqn (10).

Recovered boundary stress sensitivities

The expressions for the recovery of the complete stress tensor at the boundary were given in Bakr (1985) for axisymmetric analysis. The boundary stress sensitivities are obtained by the implicit differentiation of these boundary stress expressions as

$$\sigma_{11,L} = T_{1,L}, \quad \sigma_{12,L} = T_{2,L},$$

$$\sigma_{22,L} = \frac{\upsilon}{1-\upsilon}\sigma_{11,L} + \frac{E}{1-\upsilon^2}(e_{22,L} + \upsilon e_{\theta\theta,L}), \quad \sigma_{\theta\theta,L} = Ee_{\theta\theta,L} + \upsilon(\sigma_{11,L} + \sigma_{22,L})$$

where

$$e_{22,L} = -\frac{J_{,L}}{J^2}u_{2,s} + \frac{1}{J}u_{2,sL}$$

and

$$e_{\theta\theta,L} = \frac{1}{r^2}[u_{r,L}r - u_r r_{,L}]. \tag{15}$$

The subscripts 1 and 2 correspond, respectively, to the normal and the tangential directions of a coordinate system located at the surface. Corresponding components in the cylindrical coordinate system may be obtained by using the appropriate tensor transformation for σ_{ij}.

The evaluation of the expressions given in eqn (15) requires element displacements, tractions and their respective sensitivities. These quantities are determined as described in the previous sections.

NUMERICAL RESULTS

A set of axisymmetric test examples was solved to demonstrate the application of the above formulations using quadratic, isoparametric boundary elements. The solutions for these cases were compared to analytical results, when available, to verify the accuracy of the present method. The present implementation permits the modeling of radial cross sections with geometric configurations of a general shape. Numerical examples were chosen to include axisymmetric structures with linear, circular and hyerbolic radial geometry, respectively. The material properties considered for the following problems are: modulus of elasticity, $E = 30 \times 10^6$ psi, and Poisson's ratio, $\upsilon = 0.3$. Average values of derived sensitivities are reported for common nodes shared by two adjacent elements. All computations were done in double precision on the Ridge 3200 computer system at Worcester Polytechnic Institute.

Hollow cylinder under uniform external traction

A hollow circular cylinder subjected to a uniform pressure on its outer radius was analyzed. The geometry of the cylinder is shown in Fig. 1. The inner radius of the cylinder was chosen as the design variable for the computation of sensitivity results. Analytical expressions for this example were given by Timoshenko (1934). The exact results, obtained

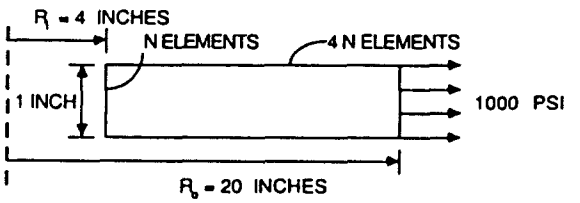

Fig. 1. Hollow cylinder under external pressure.

by performing the material derivative of these expressions, are available in the paper by Kane and Saigal (1988).

A rectangular radial section of the cylinder was discretized using axisymmetric boundary elements. Due to symmetry of this radial section only the top half of the rectangle was modeled. The line of symmetry was modeled by specifying zero displacements in the z direction along the r-axis.

The sensitivity results were obtained using a graded mesh of 30 elements ($N = 10$) as shown in Fig. 1. The geometric sensitivities were obtained through a 0.025% perturbation of the inner radius and using finite-difference relations. The values for displacement- and stress-sensitivities were given in Table 1. The analytical results for sensitivities were also shown in Table 1 for comparison. A good agreement of the present results with the analytical solution was seen.

Hollow sphere under uniform external traction

The response sensitivity solutions for the hollow sphere shown in Fig. 2 were obtained. The hollow sphere was subjected to a uniform external pressure, $P_o = 1000$ psi, and was assumed to be sensitive to changes in its inner radius, R_i. An initial inner radius, $R_i = 4$ in., and an outer radius, $R_o = 20$ in. was used. The analytical sensitivity expressions for this example may be obtained by the differentiation of the elasticity solution given in the text by Saada (1987) as

$$u_{r,L} = \frac{P_o}{2G}\left(-r_{,L}(C_1 + R_i^3/2r^3)/C_2 - r\left(\frac{3R_i^2}{2r^3}(r - R_i r_{,L})\right)\Big/ C_2 + r\left(C_1 + \frac{R_i^3}{2r^3}\right)\left(-\frac{3R_i^2}{R_o^3}\right)\Big/ C_2^2\right)$$

$$\sigma_{rr,L} = \frac{3P_o R_i^2}{C_2^2}\left[\frac{r - R_i r_{,L}}{r^4} C_2 - \frac{(1 - R_i^3/r^3)}{R_o^3}\right]$$

$$\sigma_{\theta\theta,L} = -\frac{P_o}{2C_2^2}\left[\frac{3R_i^2}{r^4}(r - R_i r_{,L})C_2 + \frac{3(2 + R_i^3/r^3)R_i^2}{R_o^3}\right]$$

Table 1. Hollow cylinder under external pressure (30 element model)

Radius (inch)	Design sensitivities: Displacement × 10^3 Analytical	Displacement × 10^3 Present	Radial stress × 10^{-1} Analytical	Radial stress × 10^{-1} Present	Hoop stress × 10^{-2} Analytical	Hoop stress × 10^{-2} Present
4.0	7.52315	7.5228	0.00000	−0.8173	0.43409	0.41331
4.3	7.51387	7.5135	−3.94616	−3.5825	0.82864	0.83800
4.7	7.44796	7.4475	−6.25734	−6.7407	1.05976	1.0477
5.0	7.34664	7.3462	−7.55208	−7.4102	1.18924	1.1927
5.3	7.22355	7.2231	−8.20584	−8.3939	1.25461	1.2499
5.7	7.08754	7.0871	−8.45219	−8.3929	1.27925	1.2806
6.0	6.94444	6.9440	−8.43943	−8.5130	1.27797	1.2760
6.3	6.79815	6.7978	−8.26323	−8.2385	1.26035	1.2608
6.7	6.65123	6.6508	−7.98611	−8.0109	1.23264	1.2319
7.0	6.50540	6.5050	−7.64927	−7.6394	1.19895	1.1991
7.3	6.36176	6.3614	−7.27999	−7.2855	1.16203	1.16175
7.7	6.22102	6.2206	−6.89639	−6.8911	1.12367	1.1239
8.0	6.08362	6.0833	−6.51042	−6.4850	1.08507	1.0853
9.0	5.69327	5.6930	−5.40302	−5.4318	0.97433	0.97345
10.0	5.33565	5.3354	−4.42708	−4.3653	0.87674	0.87822
11.0	5.00806	5.0078	−3.59516	−3.6234	0.79354	0.79273
12.0	4.70679	4.7065	−2.89352	−2.8426	0.72338	0.72462
13.0	4.42820	4.4279	−2.30250	−2.3223	0.66428	0.66368
14.0	4.16903	4.1688	−1.80318	−1.7681	0.61435	0.61520
15.0	3.92650	3.9263	−1.37924	−1.3926	0.57195	0.57154
16.0	3.69828	3.6980	−1.01725	−0.99337	0.53575	0.53633
17.0	3.48238	3.4821	−0.70630	−0.71544	0.50466	0.50437
18.0	3.27718	3.2769	−0.43760	−0.42149	0.47779	0.47818
19.0	3.08128	3.0810	−0.20407	−0.21011	0.45444	0.45422
20.0	2.89352	2.8933	0.00000	−0.01586	0.43403	0.43446

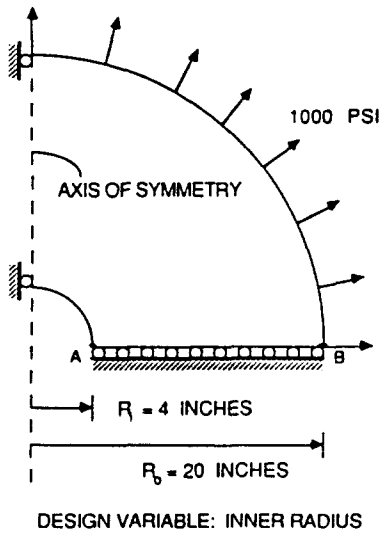

Fig. 2. Axisymmetric model of a hollow sphere.

where $C_1 = (1-2\nu)/(1+\nu)$, $C_2 = 1 - R_i^3/R_o^3$; u_r is the displacement along the radial direction, r; σ_{rr} and $\sigma_{\theta\theta}$ are the radial and circumferential stresses, respectively; G is the shear modulus; and the design variable, X_L, is the inner radius, R_i.

A radial cross-section of the sphere was modeled using 30 equally spaced elements. The centerline of the sphere is not discretized. For the field point lying on the z-axis, the singularity is treated by placing the point at a small radial distance from the axis as was done by Henry *et al.* (1987). The inner radius, R_i, was changed by 0.025% for the present computations. The results for displacement-, traction- and stress-sensitivities along the edge AB of the radial section are given in Table 2. In Table 2, the direct hoop stress sensitivities were obtained through the solution of eqn (9) whereas the derived hoop stress sensitivities were obtained using eqn (15). The analytical results obtained by using the above expressions were also given in Table 2 for comparison. The present formulations provide good prediction

Table 2. Hollow sphere under external pressure (60 element model)

	Design sensitivities						
Radius	Displacement $\times 10^5$		Radial stress		Hoop stress $\times 10^{-1}$		
(inch)	Analytical	Present	Analytical	Present	Analytical	Direct	Derived
4.0	3.61359	3.6222	0.0000	−19.302	0.91457	0.90433	0.52321
4.83	3.50135	3.5120	−88.5830	−98.454	5.34372	5.2104	5.1650
5.6	3.19249	3.2034	−94.5276	−96.972	5.64096	5.4766	5.6416
6.4	2.86818	2.8795	−81.9143	−82.322	5.01029	4.8497	5.0496
7.2	2.57325	2.5851	−66.9694	−66.837	4.26304	4.1190	4.3075
8.0	2.31489	2.3273	−53.7313	−53.515	3.60114	3.4780	3.6425
8.8	2.08995	2.1026	−42.8871	−42.724	3.05893	2.9583	3.0958
9.6	1.89305	1.9057	−34.2227	−34.147	2.62571	2.5473	2.6583
10.4	1.71899	1.7314	−27.3389	−27.346	2.28152	2.2241	2.3104
11.2	1.56336	1.5752	−21.8564	−21.931	2.00739	1.9691	2.0332
12.0	1.42262	1.4337	−17.4635	−17.586	1.78775	1.7665	1.8112
12.8	1.29395	1.3041	−13.9171	−14.070	1.61043	1.6042	1.6319
13.6	1.17513	1.1842	−11.0308	−11.200	1.46612	1.4728	1.4861
14.4	1.06439	1.0723	−8.66280	−8.8335	1.34771	1.3654	1.3666
15.2	0.960341	0.96711	−6.70458	−6.8676	1.24980	1.2768	1.2678
16.0	0.861860	0.86746	−5.07303	−5.2205	1.16823	1.2029	1.1857
16.8	0.768049	0.77250	−3.70393	−3.8299	1.09977	1.1406	1.1168
17.6	0.678182	0.68153	−2.54731	−2.6476	1.04194	1.0876	1.0587
18.4	0.591662	0.59398	−1.56403	−1.6358	0.99278	1.0418	1.0093
19.2	0.508003	0.50937	−0.72313	−0.7699	0.95073	1.0003	0.96640
20.0	0.426802	0.42732	0.00000	−0.1000	0.91457	0.94524	0.92155

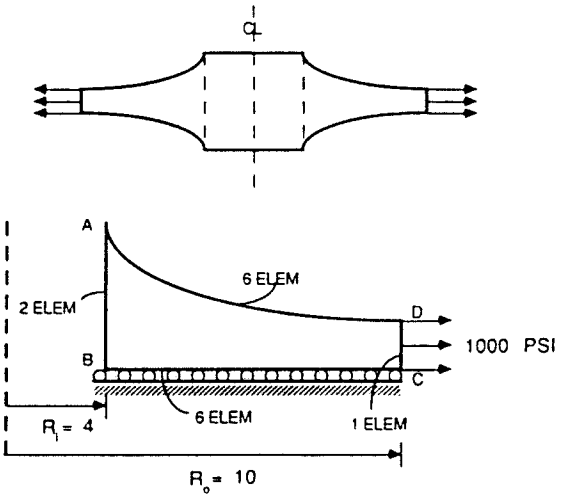

Fig. 3. Hyperbolic disk problem under external pressure.

of sensitivity results for this example using boundary elements with a circular geometric configuration.

Disk with varying thickness under uniform external pressure

A hollow circular disk with a hyperbolic variation of thickness between the inner and the outer radius was analyzed. The hyperbolic geometry in this example was modeled using quadratic boundary elements. This case was considered for the present study since the perturbation of the inner radius, R_i, provides a more general input for the geometric sensitivity. This input also includes the variation of normals at the nodal points in addition to the variation of their coordinates. The geometry resembles that of an aircraft turbine disk and is of practical significance.

A radial cross-section of the hyperbolic disk was modeled using two different meshes of 15 and 30 boundary elements, respectively. The number of elements used on each side for the 15-element model are shown in Fig. 3. These elements were doubled on each side for the 30-element model. The design variable, R_i, was perturbed by 0.025% and the edges AB, BC, and AD were remeshed for the sensitivity computations. The sensitivity results for displacement sensitivities and their convergence with a refined mesh consisting of 30 elements are given in Table 3. This table also shows the radial- and circumferential-stress sensitivities for the 30 element model. The sensitivity results for displacements and recovered stresses are given in Table 3. The analytical results obtained from the differentiation of the elasticity solution given in Saada (1987) are also given in Table 3. A state of plane stress was assumed in the elasticity solution which leads to a constant stress through the thickness for any circumferential section. This assumption was not made in the present analysis, however. The results shown in Table 3 are then in good agreement and demonstrate the validity of the present formulations for a more general, curved geometry.

Notched cylindrical bar under axial tension

A notched bar with geometry as shown in Fig. 4 was used to determine the axial stress sensitivities due to the notch radius, R_c. The bar is subjected to an axial tension of 1000 psi. This example has previously been considered by Bakr (1985) for stress analysis using boundary elements. In the present study, only one half of the solid bar cross-section was modeled using 21, 42 and 84 elements, respectively. Again, to avoid singularities due to the field point lying on the centerline, the centerline was not discretized. The meshes provided are sufficiently refined to take account of the high stress concentrations in the vicinity of the notches. The axial stress sensitivities were obtained at the stress concentration location A using the three respective meshes. This location on the cylindrical bar has a stress concentration factor of approximately 6 for the geometry shown. The results for the

Table 3. Circular disk with hyperbolic varying thickness

Radius (inch)	Design sensitivities: Displacement × 10^5 Saada (1987)	Displacement × 10^5 Model A	Displacement × 10^5 Model B	Hoop stress × 10^{-2} Saada (1987)	Hoop stress × 10^{-2} Model B
4.00	9.47321	9.2630	9.2656	3.61679	3.1885
4.25	9.42680	—	9.1888	3.70837	3.6148
4.50	9.35745	9.0977	9.1002	3.72962	3.5803
4.75	9.27133	—	9.0059	3.70413	3.5739
5.00	9.17287	8.9071	8.9089	3.64779	3.5131
5.25	9.06521	—	8.8101	3.57141	3.4410
5.50	8.95065	8.7085	8.7095	3.48243	3.3595
5.75	8.83086	—	8.6068	3.38600	3.2700
6.00	8.70705	8.5013	8.5015	3.28567	3.1798
6.25	8.58009	—	8.3932	3.18392	3.0864
6.50	8.45064	8.2820	8.2817	3.08243	2.9946
6.75	8.31914	—	8.1669	2.98237	2.9032
7.00	8.18594	8.0496	8.0491	2.88450	2.8140
7.25	8.05124	—	7.9285	2.78934	2.7274
7.50	7.91522	7.8060	7.8054	2.69719	2.6433
7.75	7.77796	—	7.6802	2.60821	2.5628
8.00	7.63952	7.5539	7.5531	2.52248	2.4861
8.25	7.49994	—	7.4242	2.43999	2.4130
8.50	7.35919	7.2943	7.2934	2.36071	2.3458
8.75	7.21729	—	7.1600	2.28455	2.2801
9.00	7.07419	7.0238	7.0231	2.21142	2.2205
9.25	6.92986	—	6.8816	2.14119	2.1579
9.50	6.78426	6.7372	6.7360	2.07374	2.0889
9.75	6.63734	—	6.5900	2.00896	2.0146
10.00	6.48906	6.0526	6.4515	1.94672	1.9407

† Plane Stress Solution
Model A consists of 15 boundary elements, and
Model B consists of 30 boundary elements

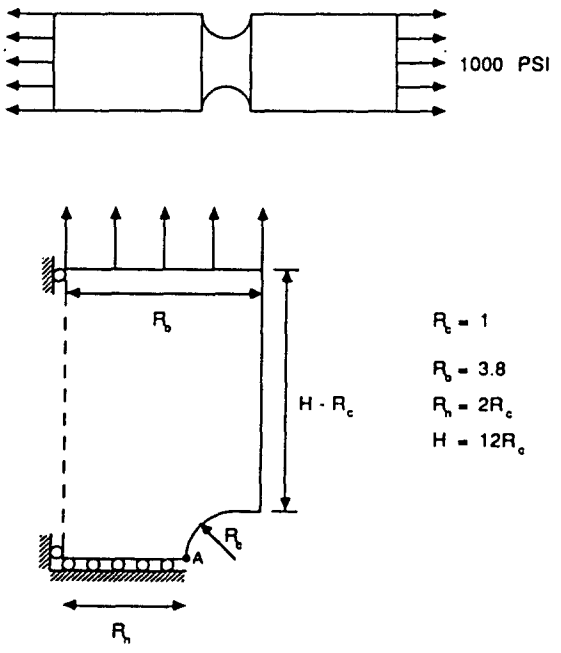

DESIGN VARIABLE: NOTCH RADIUS, R_c

Fig. 4. Notched cylindrical bar under axial stress.

Table 4. Sensitivities of a notched cylindrical bar under axial tension at stress concentration location

	Number of elements		
	21	42	84
Axial stress $\times 10^{-3}$ (psi)	6.2558	6.3462	6.3848
Axial stress sensitivity $\times 10^{-3}$	3.0614	2.8661	2.8016
Radial displacement $\times 10^{5}$ (inches)	−2.3715	−2.3318	−2.2875
Radial displacement sensitivity $\times 10^{5}$	3.8123	3.8130	3.8128

displacement, axial stress, and the corresponding sensitivities are shown in Table 4. A convergence of the sensitivity results similar to that for the analysis results was obtained using the present meshes.

CONCLUSIONS

This paper presents an implicit differentiation formulation for the design sensitivity analysis of axisymmetric elastic continua. The kernel functions for axisymmetric sensitivity matrices are presented. The integration of these differentiated kernel functions as well as the evaluation of the singular terms of sensitivity matrices based on the rigid body mode and the inflation mode are discussed. The equations for recovery of boundary stress sensitivities using the results of the design sensitivity analysis are given. Numerical results for a wide class of axisymmetric problems with available analytical solutions are provided to demonstrate the accuracy of the present approach. Additional examples show the versatility of the method in predicting design sensitivities of problems with a general geometry and stress concentration.

Acknowledgements—This research was supported under NSF grant MSM 8707842. Dr A. Kobayashi is the project monitor for this grant. The help of Professor P. K. Banerjee in providing his continuous boundary element analysis program is sincerely appreciated.

REFERENCES

Bakr, A. A. (1985). *The Boundary Integral Equation Method in Axisymmetric Stress Analysis Problems*. Springer, Berlin.

Banerjee, P. K. and Butterfield, R. (1981). *Boundary Element Methods in Engineering Science*. McGraw-Hill, U.K.

Barone, M. R. and Yang, R. J. (1988). Boundary integral equations for recovery of design sensitivities in shape optimization. *AIAA Jnl* **26**, 589–594.

Brebbia, C. A., Telles, J. C. F. and Wrobel, L. C. (1984). *Boundary Element Techniques*. Springer, Berlin.

Cruse, T. A., Snow, D. W. and Wilson, R. B. (1977). Numerical solutions in axisymmetric elasticity. *Comput. Struct.* **7**, 445–451.

Henry, D. P., Pape, D. A. and Banerjee, P. K. (1987). New axisymmetric formulation for body forces using particular integrals. *J. Engng. Mech.* **113**, 671–688.

Kane, J. H., and Saigal, S. (1988). Design sensitivity analysis of solids using BEM. *J. Engng Mech.* **114**, 1703–1722.

Mota Soares, C. A. and Choi, K. K. (1986). Boundary elements in shape optimal design of structures. In *The Optimum Shape*, International Symposium, General Motors Research Labs, Warren, Michigan (Edited by J. A. Bennett and M. E. Botkin). Plenum Press, New York.

Saada, A. S. (1987). *Elasticity, Theory and Applications*. Malabar, FL.

Saigal, S. and Kane, J. H. (1989). A boundary element shape optimization system for aircraft components. *AIAA Jnl* (to appear).

Saigal, S., Aithal, R. and Kane, J. H. (1989). Conforming boundary elements in plane elasticity for shape design sensitivity. *Int. J. Numer. Meth. Engng* (to appear).

Sarihan, V. and Mukherjee, S. (1982). Axisymmetric viscoplastic deformation by the boundary element method. *Int. J. Solids Struct.* **18**, 1113–1128.

Timoshenko, S. (1934). *Theory of Elasticity*. McGraw-Hill, New York.

Wu, S. J. (1986). Applications of the boundary element method for structural shape optimization. Ph.D. thesis, University of Missouri, Columbia.

APPENDIX

The sensitivities of the kernel functions are written as

$$U_{rr_\perp} = C_1\{U_{rr1_\perp}EI_1 + U_{rr1}EI_{1_\perp} - U_{rr2_\perp}EI_2 - U_{rr2}EI_{2_\perp}\}$$
$$U_{rz_\perp} = C_1\{U_{rz1_\perp}EI_1 + U_{rz1}EI_{1_\perp} - U_{rz2_\perp}EI_2 - U_{rz2}EI_{2_\perp}\}$$
$$U_{zr_\perp} = -C_1\{U_{zr1_\perp}EI_1 + U_{zr1}EI_{1_\perp} - U_{zr2_\perp}EI_2 - U_{zr2}EI_{2_\perp}\}$$
$$U_{zz_\perp} = 2C_1\{U_{zz1_\perp}EI_1 + U_{zz1}EI_{1_\perp} - U_{zz2_\perp}EI_2 - U_{zz2}EI_{2_\perp}\},$$

where

$$U_{rr1} = \frac{(3-4\upsilon)(r^2+R^2+\bar{z}^2)+\bar{z}^2}{RQ}, \qquad U_{rr2} = \frac{(3-4\upsilon)Q^2+\bar{z}^2(r^2+R^2+\bar{z}^2)/D^2}{RQ}$$

$$U_{rz1} = \frac{\bar{z}}{Q}, \qquad U_{rz2} = \bar{z}\left[\frac{R^2-r^2+\bar{z}^2}{D^2Q}\right], \qquad U_{zr1} = \frac{r\bar{z}}{RQ}, \qquad U_{zr2} = \bar{z}r\left[\frac{r^2-R^2+\bar{z}^2}{RD^2Q}\right]$$

$$U_{zz1} = \left[\frac{(3-4\upsilon)r}{Q}\right], \qquad U_{zz2} = \left[\frac{r\bar{z}^2}{D^2Q}\right]$$

$$U_{rr1_\perp} = 2[(3-4\upsilon)(rr_\perp + RR_\perp + \bar{z}\bar{z}_\perp) + \bar{z}\bar{z}_\perp]/RQ - [(3-4\upsilon)(r^2+R^2+\bar{z}^2)+\bar{z}^2][R_\perp Q + RQ_\perp]/R^2Q^2$$

$$U_{rr2_\perp} = 2[(3-4\upsilon)QQ_\perp + (\bar{z}\bar{z}_\perp D - \bar{z}^2D_\perp)(r^2+R^2+\bar{z}^2)/D^3 + \bar{z}^2(rr_\perp + RR_\perp + \bar{z}\bar{z}_\perp)/D^2]/RQ$$
$$- [(3-4\upsilon)Q^2 + \bar{z}^2(r^2+R^2+\bar{z}^2)/D^2][R_\perp Q + RQ_\perp]/R^2Q^2$$

$$U_{rz1_\perp} = \frac{\bar{z}_\perp Q - \bar{z}Q_\perp}{Q^2}$$

$$U_{rz2_\perp} = \bar{z}_\perp\left[\frac{R^2-r^2+\bar{z}^2}{D^2Q}\right] + \bar{z}\frac{2(RR_\perp - rr_\perp + \bar{z}\bar{z}_\perp)D^2Q - (R^2-r^2+\bar{z}^2)(2DD_\perp Q + D^2Q)}{D^4Q^2}$$

$$U_{zr1_\perp} = (r_\perp\bar{z} + r\bar{z}_\perp)/RQ - (r\bar{z})(R_\perp Q + RQ_\perp)/R^2Q^2$$

$$U_{zr2_\perp} = (\bar{z}_\perp r + \bar{z}r_\perp)\left[\frac{r^2-R^2+\bar{z}^2}{RD^2Q}\right] + 2\bar{z}r\left[\frac{rr_\perp - RR_\perp + \bar{z}\bar{z}_\perp}{RD^2Q}\right] - \bar{z}r\frac{(r^2-R^2+\bar{z}^2)(R_\perp D^2Q + 2RDD_\perp Q + RD^2Q_\perp)}{R^2D^4Q^2}$$

$$U_{zz1_\perp} = \frac{(3-4\upsilon)r_\perp Q - (3-4\upsilon)rQ_\perp}{Q^2}$$

$$U_{zz2_\perp} = \frac{(r_\perp\bar{z}^2 + 2r\bar{z}\bar{z}_\perp)D^2Q - (r\bar{z}^2)(2DD_\perp Q + D^2Q_\perp)}{D^4Q^2}.$$

The traction kernel sensitivities are given as

$$T_{rr_\perp} = 2\mu\{T_{rr1_\perp}n_r + T_{rr1}n_{r_\perp} + T_{rr2_\perp}n_z + T_{rr2}n_{z_\perp}\}$$
$$T_{rz_\perp} = 2\mu\{T_{rz1_\perp}n_r + T_{rz1}n_{r_\perp} + T_{rz2_\perp}n_z + T_{rz2}n_{z_\perp}\}$$
$$T_{zr_\perp} = 2\mu\{T_{zr1_\perp}n_r + T_{zr1}n_{r_\perp} + T_{zr2_\perp}n_z + T_{zr2}n_{z_\perp}\}$$
$$T_{zz_\perp} = 2\mu\{T_{zz1_\perp}n_r + T_{zz1}n_{r_\perp} + T_{zz2_\perp}n_z + T_{zz2}n_{z_\perp}\},$$

where

$$T_{rr1} = \frac{1-\upsilon}{1-2\upsilon}U_{rr,r} + \frac{\upsilon}{1-2\upsilon}\left(\frac{U_{rr}}{r} + U_{zr,z}\right)$$

$$T_{rz1} = \frac{1-\upsilon}{1-2\upsilon}U_{rz,r} + \frac{\upsilon}{1-2\upsilon}\left(\frac{U_{rz}}{r} + U_{zz,z}\right), \quad T_{rz2} = \tfrac{1}{2}(U_{rr,z} + U_{zr,r})$$

$$T_{zr1} = \frac{1-\upsilon}{1-2\upsilon}U_{zr,z} + \frac{\upsilon}{1-2\upsilon}\left(\frac{U_{zr}}{r} + U_{rr,r}\right), \quad T_{zr2} = \tfrac{1}{2}(U_{rr,z} + U_{zz,r})$$

$$T_{zz1} = \frac{1-\upsilon}{1-2\upsilon}U_{zz,z} + \frac{\upsilon}{1-2\upsilon}\left(\frac{U_{rz}}{r} + U_{rz,r}\right), \quad T_{zr2} = T_{rz2} = \tfrac{1}{2}(U_{rr,z} + U_{zr,r})$$

$$T_{zz2} = \tfrac{1}{2}(U_{rz,z} + U_{zz,r}) = T_{rz2}$$

$$T_{rr1_\perp} = \frac{1-\upsilon}{1-2\upsilon}U_{rr,r_\perp} + \frac{\upsilon}{1-2\upsilon}\left(\frac{U_{rr_\perp}r - U_{rr}r_\perp}{r^2} + U_{zr,z_\perp}\right), \quad T_{rz2_\perp} = \tfrac{1}{2}(U_{rr,z_\perp} + U_{zr,r_\perp})$$

$$T_{rr1_L} = \frac{1-\upsilon}{1-2\upsilon} U_{rr_L} + \frac{\upsilon}{1-2\upsilon}\left(\frac{U_{rr_L}}{r} - \frac{U_{rr}r_{,L}}{r^2} + U_{\theta\theta_L}\right), \quad T_{rr2_L} = \tfrac{1}{2}(U_{rr_L} + U_{zz_L})$$

$$T_{\theta\theta 1_L} = \frac{1-\upsilon}{1-2\upsilon} U_{\theta\theta_L} + \frac{\upsilon}{1-2\upsilon}\left(\frac{U_{rr_L}}{r} - \frac{U_{rr}r_{,L}}{r^2} + U_{rr_L}\right)$$

$$T_{zz1_L} = \frac{1-\upsilon}{1-2\upsilon} U_{zz,L} + \frac{\upsilon}{1-2\upsilon}\left(\frac{U_{rr_L}}{r} - \frac{U_{rr}r_{,L}}{r^2} + U_{rr_L}\right)$$

$$T_{\theta\theta 2_L} = T_{rr2_L}, \quad T_{zz2_L} = T_{rr2_L}$$

$\bar{z} = z - Z$, $Q^2 = (r+R)^2 + (\bar{z})^2$, $D^2 = (r-R)^2 + (\bar{z})^2$

$$Q_{,L} = \frac{1}{Q}[(r+R)(r_{,L} + R_{,L}) + \bar{z}\bar{z}_{,L}], \quad D_{,L} = \frac{1}{D}[(r-R)(r_{,L} - R_{,L}) + \bar{z}\bar{z}_{,L}].$$

(R, Z) and (r, z) are the coordinates of the load point, and the Gauss point on the body, respectively; EI_1 and EI_2 are the elliptic integrals of the first and second kind, respectively.